Mansoura University
Faculty of Engineering
Mansoura Engineering Journal

Numerical and Experimental Study of Water Hammer in Viscoelastic Pipes with and without Extended Partial Blockage

دراسة عددية وعملية للطرق المائي في مواسير بلاستيكية مع وبدون انسداد جزئي ممتد

Ahmed T. Nile, Berge Djebedjian and Mohamed El-Naggar

KEYWORDS:
Water hammer, method of characteristics, viscoelastic pipes, extended partial blockage.

الملخص العربي : يقدم البحث حل لمعادلتي الاستمرارية وبقاء كمية الحركة باستخدام طريقة الصفات المميزة (Method of Characteristics) لمحاكاة ظاهرة الطرق المائي في المواسير البلاستيكية، مع الأخذ في الاعتبار تأثير السلوك الميكانيكي لجدران الأنبوب (Viscoelasticity) والاحتكاك غير المستقر (Unsteady Friction). ولدراسة تأثير وجود أنبوب ذو قطر مختلف مع القطر الرئيسى فقد تم عمل نموذج ليحاكي ظاهرة الطرق المائي سواء في أنبوب واحد ذو قطر ثابت، أو في حالة وجود أنبوب بقطر مختلف مع الأنبوب الرئيسي. ولأهمية الدور الذي تلعبه الظروف الحدية في تحديد شكل موجة الضغط الناشئة، فقد تم سردها في هذا البحث. وقد تمت مقارنة نتائج النموذج العددية مع نتائج تجارب معملية سابقة. بالإضافة لذلك ، فقد تم تجهيز تجربة معملية لمقارنة النتائج العددية الخاصة بالنموذج الرياضي مع نتائج تلك التجربة المعملية. وقد أظهرت مقارنة النتائج العددية مع النتائج المعملية أن النموذج قد تنبأ بشكل جيد بشكل موجة الضغط المتولدة في الأنبوب ذو القطر الثابت، أما في حالة وجود أنبوب ذو قطر مختلف مع الأنبوب الرئيسي ، فقد تنبأ النموذج بشكل جيد إلى حد ما بالنتائج في أول ذروتين للضغط ثم بعد ذلك أظهرت النتائج وجود إزاحة في الطور من بعد الذروة الثانية وهذه الإزاحة تزداد مع الزمن. وفى النهاية ، يعرض البحث دراسة عددية لدراسة تأثير بعض المتغيرات الهامة على شكل موجة الضغط المتولدة.

***Abstract*— In the present paper, the continuity and momentum equations were solved using the Method of Characteristics to simulate the water hammer phenomenon taking into account the effect of pipe wall viscoelasticity and unsteady friction of fluid flow. In order to study the effect of extended blockage existence in the pipeline, a MATLAB code was developed to deal with both cases: simple single pipeline and compound series pipes. Because of the vital role that boundary conditions play in the profile of the generated pressure wave, they were mentioned in this paper. Code developed was validated with previous experimental data for the case of single pipe and for compound pipeline. In addition to that, a simple Reservoir-Pipe-Valve test rig was constructed using PVC pipe. The experimental data extracted from the test rig were compared with the numerical results of the code for both simple and complex pipelines. The code could predict the pressure head fluctuations quite accurately in the case of simple pipe. However, in case of complex series pipeline, it could predict the maximum pressure head for the first two peaks, but a phase shift was noticed after the second peak and progressively increased with time. Finally, a sensitivity analysis was carried out to investigate the effect of changing some essential parameters on the pressure wave profile.**

Received: (27 June, 2018) - Accepted: (19 September, 2018)

Ahmed T. Nile is with Mechanical Power Engineering Department, Faculty of Engineering, Mansoura University, El-Mansoura 35516, Egypt (e-mail: ahmed_nile@mans.edu.eg).

Berge Djebedjian is with Mechanical Power Engineering Department, Faculty of Engineering, Mansoura University, El-Mansoura 35516, Egypt (e-mail: bergedje@mans.edu.eg).

Mohamed El-Naggar is with Mechanical Power Engineering Department, Faculty of Engineering, Mansoura University, El-Mansoura 35516, Egypt (e-mail: naggarm@mans.edu.eg).

NOMENCLATURE

A	Pipe cross-sectional area,	$[m^2]$
a	Pressure wave celerity, $a=\sqrt{(K/\rho)/\left[1+(K/E)(D/e)\psi\right]}$,	$[m/s]$
D	Pipe internal diameter,	$[m]$
E	Young's modulus of pipe wall material,	$[Pa]$
e	Pipe wall thickness,	$[mm]$

f	Darcy-Weisbach friction factor
g	Gravitational acceleration, [m/s^2]
H	Pressure head, [m]
H_L	Pressure head at node L, [m]
H_P	Pressure head at node P, [m]
H_R	Pressure head at node R, [m]
H_{Res}	Reservoir head, [m]
h_L	Head loss, [m]
J	Creep compliance function, [Pa^{-1}]
K	Bulk modulus for water, [Pa]
k_{ball}	Ball valve minor loss coefficient
k_{bend}	Bend minor loss coefficient
$k_{contraction}$	Abrupt contraction minor loss coefficient
k_{ent}	Pipe entrance loss coefficient
k_{exit}	Pipe exit loss coefficient
$k_{expansion}$	Abrupt expansion minor loss coefficient
k_s	Solenoid valve minor loss coefficient when fully opened, $k_s = 9.5788$
L	Pipe length, [m]
L_1	First pipe length, [m]
L_2	Second pipe length, [m]
L_3	Third pipe length, [m]
m_i	Coefficient of the ith approximating term of weighting function
N	Number of terms in the approximate weighting function
n_i	Coefficient in exponent of ith approximating term of weighting function
Q	Discharge, [m^3/s]
Re	Reynolds number, $\mathrm{Re} = VD/\nu$
t	Time, [s]
t_c	Valve closure time, [s]
V	Fluid velocity, [m/s]
V_0	Fluid velocity at steady state conditions, [m/s]
V_L	Fluid velocity at node L, [m/s]
V_P	Fluid velocity at node P, [m/s]
V_R	Fluid velocity at node R, [m/s]
$\dot{V}$	Mean acceleration in pipe, [m/s^2]
x	Axial coordinate
Y_{ai}	ith contribution to approximation of the historical integral, [m/s]

Greek letters

Δt	Time step, [s]
ε_r	Retardation strain
ν	Fluid kinematic viscosity, [m^2/s]
ρ	Fluid density, [kg/m^3]
σ	Stress, [Pa]
τ_s	Steady shear stress, [N/m^2]
τ_u	Unsteady shear stress, [N/m^2]
τ_w	Wall shear stress, [N/m^2]
υ	Poisson's ratio
ψ	Parameter depends on the pipe geometry and constraint conditions

I. Introduction and Literature Review

WATER hammer is one of the common phenomenon which related to pipelines. That phenomenon depends on the momentum of the flowing fluid. When the fluid's momentum changes suddenly, i.e. due to the fast valve closure, fast valve opening, shut off of pump or demands fluctuate at any part of the pipeline network, water hammer aroused. All of those causes need force either to accelerate or decelerate the fluid. That force magnitude depends on how much that momentum changes and it appears throughout the pipeline networks as hydraulic pressure transient. In case of rapid changes, a huge pressure generated and that may lead to pipeline damage.

The viscoelasticity of a pipe wall material means that it has characteristics of both fluid "in its viscous behavior" and solid "in its elastic behavior". It also means that the mechanical properties "such as stress and strain" are a time function and this is due to its molecular structure. Therefore, the behavior of pipes made of polymers is different from those made of steel or concrete.

On the other hand, water hammer has useful applications such as blockage detection. Studying the effect of blockage existence in viscoelastic pipes was first studied by **Meniconi et al. [1]**. They presented experimental and numerical data concerning the interaction between an incident pressure wave and partial blockage (a valve, a single pipe contraction or expansion and a series of pipe contraction/expansion). They figured out, from experimental tests, for partial blockages the smaller the length, the more intense the overlapping of pressure waves due to the expansion and contraction in series.

Massari et al. [2] developed a stochastic model for detecting partial blockages in viscoelastic pipeline using transients. Based on numerical and experimental case studies, it was found that, a first good estimation can be obtained by a single transient event using fast valve closure to locate and size blockages in simple pipelines.

Finally, **Meniconi et al. [3]** used laboratory and numerical tests to analyze the mechanism of interaction between an incident pressure wave and discrete blockages with different geometrical characteristics concerning viscoelastic pipes. They used a partially closed in-line butterfly and ball valves to simulate a sinuous pressure wave path (type I mechanism) and small bore pipes for a straight pressure wave path (type II mechanism). They found that type II mechanism of interaction evolves towards type I mechanism for larger pre-transient Reynolds number.

Concerning the literature review of the sensitivity analysis of water hammer in pipelines, **Emadi and Solemani [4]** used WaterGEMS Software to simulate Kuhrang Pumping Station, Iran, where 200 lit/s of water were pumped with 194 m dynamic head through 1.5 kilometers steel pipe to transport it to Cheshme Morvarid for farmland irrigation. They found that decreasing the internal diameter of the pipe as well as increasing either pipe wall thickness or water temperature increases the pressure wave celerity and so the maximum water hammer pressure head. They investigated also replacing the steel pipe with pipe has lower Young's modulus and Poisson ratio (like Glass Reinforces pipe) and they found that it decreased the maximum water hammer water column.

Mansuri et al. [5,6] used the MATLAB software to simulate the water hammer in simple pipeline. Then, they investigated the effect of increasing the pipe roughness as well as decreasing the pipeline length and increasing the pipe internal diameter which led to a reduction in pressure fluctuation range.

Throughout the present paper, the governing equations describing the water hammer phenomenon in viscoelastic pipes are solved by using the Method of Characteristics (MOC). A MATLAB code **[7]** is developed to solve the equations resulted from the (MOC) for single pipeline and for

multiple pipes in series. According to the literature review, **Meniconi et al. [1]** used pipes made of high density polyethylene unlike herein, a polyvinyl chloride pipes were used. In addition, **Meniconi et al. [1]** used an unsteady friction model different from that was used in the present study. The boundary condition equations used in the developed code are stated in the mathematical model. Then, the code is validated with experimental data extracted from previous work and with experimental data obtained from the test rig constructed at the Hydraulic Machines Laboratory, Faculty of Engineering, Mansoura University. By the end of the paper, a sensitivity analysis is carried out to investigate the effect of some essential parameters related to the water hammer phenomenon. Form the literature review, the sensitivity analysis carried out by **Emadi and Solemani [4]** and **Mansuri et al. [5,6]** concerning single elastic pipe, but in the present paper the sensitivity analysis was performed for viscoelastic pipes for two cases: 1. Single pipe and 2. Three pipes in series (Partial blockage).

II. MATHEMATICAL MODEL

A. Governing Equations

The principle equations used to simulate water hammer in viscoelastic pipeline are illustrated. For one-dimensional flow, the continuity and momentum equations are (**Covas et al. [8]**):

Continuity equation:

$$\frac{g}{a^2}\frac{dH}{dt}+\frac{\partial V}{\partial x}+2\frac{d\varepsilon_r(t)}{dt}=0 \tag{1}$$

Momentum equation:

$$g\frac{\partial H}{\partial x}+\frac{dV}{dt}+\frac{4}{\rho}\frac{\tau_w}{D}=0 \tag{2}$$

Those equations are valid under the following circumstances: 1. One-dimensional flow, which means that the characteristics such as flow velocity and pressure head are averaged at each cross section. 2. The fluid is Newtonian, homogenous, always exists in liquid phase, completely filling the pipeline and slightly compressible without significant change in its density. 3. The pipe is horizontal with a circular cross-sectional area of diameter *D* and wall thickness *e*, which is small compared with pipe diameter. 4. The pipe wall material is isotropic and exhibits a linear viscoelastic behavior, for small strains, and it has a constant Poisson ratio, so the mechanical behavior is only dependent on a creep-function. 5. Head loss during the transient event is estimated due to both steady and unsteady friction.

The retardation strain rate term is given by **Keramat et al. [9]**:

$$\begin{aligned}\frac{d\varepsilon_r(t)}{dt}&=\frac{d}{dt}\int_0^t\sigma(t-\tau')\frac{\partial J(\tau')}{\partial\tau'}d\tau'\\&=\frac{\rho g D}{2e}\left(1-\upsilon^2\right)\int_0^t\frac{d}{dt}H(t-\tau')\frac{\partial J(\tau')}{\partial\tau'}d\tau'\end{aligned} \tag{3}$$

The wall shear stress, τ_w , is decomposed into two terms:

$$\tau_w=\tau_s+\tau_u \tag{4}$$

where, τ_s represents the wall shear stress calculated based on quasi-steady flow model, and τ_u represents the wall shear stress calculated based on unsteady flow model.

In terms of the Darcy-Weisbach friction factor, *f*, the quasi-steady wall shear stress can be calculated from:

$$\tau_s=\frac{\rho f}{8}V(t)\left|V(t)\right| \tag{5}$$

For unsteady friction model, **Vardy and Brown [10]** approximation is used. Defining the wall shear stress τ_u at an instant,

$$\tau_u(t+\Delta t)\approx\frac{4\rho\nu}{D}\cdot\sum_{i=1}^{N}\left[Y_{ai}(t)e^{-\left(4n_i\nu/D^2\right)\Delta t}+\frac{m_i\dot{V}R^2}{n_i\nu}\left(1-e^{-\left(4n_i\nu/D^2\right)\Delta t}\right)\right] \tag{6}$$

where,

$$Y_{ai}(t)=Y_{ai}(t-\Delta t)e^{-\left(4n_i\nu/D^2\right)\Delta t}+\frac{m_i\dot{V}D^2}{4n_i\nu}\left(1-e^{-\left(4n_i\nu/D^2\right)\Delta t}\right) \tag{7}$$

$$\dot{V}=\frac{V(t+\Delta t)-V(t)}{\Delta t} \tag{8}$$

The values of constants n_i and m_i are listed in Table 1.

TABLE 1.
VALUES OF CONSTANTS n_i AND m_i, VARDY AND BROWN [10]

	Laminar flow		Smooth-wall turbulent flow	
i	n_i	m_i	n_i	m_i
1	26.3744	1	10^3	0.15238
2	10^2	2.1830	$10^{3.5}$	16.20975
3	$10^{2.5}$	2.7140	10^4	27.30278
4	10^3	7.5455	10^5	126.2398
5	10^4	39.0066	10^6	336.4545
6	10^5	106.8075	10^7	1137.951
7	10^6	359.0847	10^8	3500.676
8	10^7	1107.9295	10^9	11200.46
9	10^8	3540.6830		

B. Method of Characteristics

In the previous section, the continuity and momentum equations are presented, and as shown in equations (1) and (2), they are a pair of quasi-linear hyperbolic partial differential equations in terms of the two dependent variables (flow velocity and pressure head) and two independent variables (distance along the pipe and time). Those equations are transformed to four ordinary differential equations using the method of characteristics (**Fox [11], Watters [12], Wylie and Streeter [13], Larock et al. [14]** and **Chaudhry [15]**), which are:

For characteristic line C^+:

$$\frac{dV}{dt}+\frac{g}{a}\frac{dH}{dt}+\frac{4}{\rho}\frac{\tau_w}{D}+2\frac{d\varepsilon_r(t)}{dt}=0 \tag{9}$$

$$\frac{dx}{dt} = V + a \tag{10}$$

For characteristic line C^-:

$$\frac{dV}{dt} - \frac{g}{a}\frac{dH}{dt} + \frac{4}{\rho}\frac{\tau_w}{D} - 2\frac{d\varepsilon_r(t)}{dt} = 0 \tag{11}$$

$$\frac{dx}{dt} = V - a \tag{12}$$

From equations (10) and (12), the time step must satisfy the following relation:

$$\Delta t = \frac{\Delta x}{max\left|V + a\right|} \tag{13}$$

Using the finite difference approximation to equations (9) and (11) and multiplying each one by Δt and imply interpolation method to assure accurate and stable numerical solution, the equations are:

For characteristic line C^+:

$$(V_P - V_L) + \frac{g}{a}(H_P - H_L) + \frac{4}{\rho}\frac{\tau_w}{D}\Delta t + 2\frac{d\varepsilon_r(t)}{dt}\Delta t = 0 \tag{14}$$

For characteristic line C^-:

$$(V_P - V_R) - \frac{g}{a}(H_P - H_R) + \frac{4}{\rho}\frac{\tau_w}{D}\Delta t - 2\frac{d\varepsilon_r(t)}{dt}\Delta t = 0 \tag{15}$$

The x-t grid of characteristic lines C^+ and C^- for any point P is illustrated in Fig. 1.

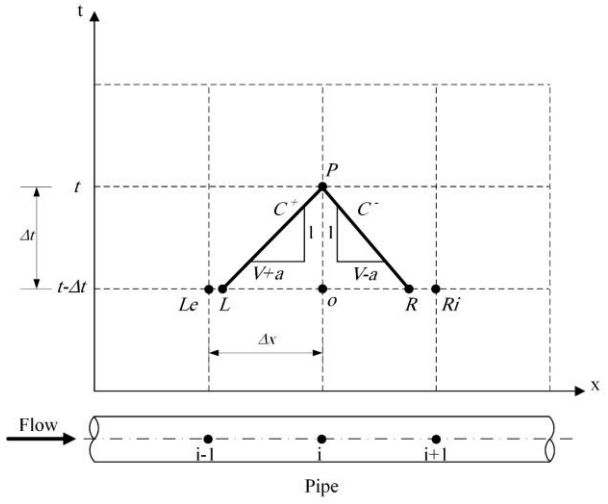

Fig. 1. Characteristic grid

C. Boundary Conditions

The boundary conditions for each pipe play a vital role in simulating water hammer, so it must be studied carefully. At any boundary, there is only one compatibility equation so another equation should be stated to be able to calculate both pressure head and flow velocity at this boundary. Some types of boundaries are illustrated and the corresponding equations are deduced.

1. *Reservoir at upstream end of the pipe*

Considering that the reservoir is located at the upstream end of the pipe and assuming that its level H_{Res} does not change during the transient event.

Applying Bernoulli equation between the free surface of the reservoir and point *i* as shown in Fig. 2:

$$H_{Res} = H_P + (1 + k_{ent})\frac{V_P^2}{2g} \tag{16}$$

Solving this equation with compatibility equation, C^-, the pressure head and flow velocity at point P are estimated.

For reversal flow: the energy equation is,

$$H_P + \frac{V_P^2}{2g} = H_{Res} + k_{exit}\frac{V_P^2}{2g} \tag{17}$$

where $k_{exit} = 1$ (all kinetic energy is lost in the reservoir), and therefore:

$$H_P = H_{Res} \tag{18}$$

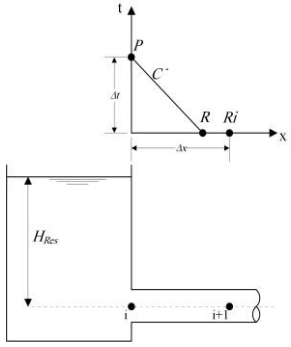

Fig. 2. Characteristic line for reservoir at upstream end

2. *Valve at downstream end of the pipe*

Figure3 shows the characteristic line at the valve and just C^+ equation is existed at that boundary. To get the value of the flow velocity and pressure head at point *P*, another equation should be used. This equation is stated depending on one of the following two assumptions:

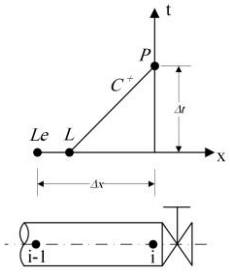

Fig. 3. Characteristic line for a valve at downstream end

(1) *Linear velocity variation model*

The decrease of the flow velocity through a valve during closure can be expressed as a linear function. If the closure time of the valve is t_c and the steady flow velocity V_0, so the flow velocity during any time t can be calculated from,

$$V_P = \begin{cases} V_0\left(1-\dfrac{t}{t_c}\right) & \text{when } t \le t_c \\ 0 & \text{when } t > t_c \end{cases} \quad (19)$$

(2) ***Actual model***

During water hammer due to valve closure, an increasing head loss is generated in the pipeline system, so the flow begins to decelerate. The following equation is expressing the head loss across the solenoid valve during steady flow:

$$h_L = k_s \frac{V^2}{2g} \quad (20)$$

where k_s is the minor loss coefficient of the solenoid valve when it is fully opened and V is the flow velocity. When the valve begins to close, the value of the minor loss coefficient increases according to a function that depends on the closure time and closing maneuvering which differs from one valve to another. Therefore, the energy equation across the valve "discharging into atmosphere" is:

$$H_P = k_s(t)\frac{V_P^2}{2g} \quad (21)$$

Considering the present experimental work, Eq. (21) is modified to take into account the value of the minor loss coefficient of a ball valve located downstream the solenoid valve, the equation becomes

$$H_P = \left(k_s(t) + k_{ball}\right)\frac{V_P^2}{2g} \quad (22)$$

and k_{ball} is determined from the steady flow conditions and its value is constant during the transient event.

The calculation of the pressure head and the flow velocity at the valve is achieved by using one of the aforementioned models, Eq. (19) or (22), and solving it with the C^+ equation.

3. ***Series junction***

This case is a common case that exists in almost all networks. In the case of two pipes meeting together at a junction, Fig. 4, the upstream pipe meets the downstream pipe at its upstream end at the *n*th node.

At this junction, both mass and energy balance must be satisfied:

Continuity equation:

$$V_n A_{upstream\ pipe} = V_1 A_{downstream\ pipe} \quad (23)$$

Energy equation:

$$H_n + \frac{V_n^2}{2g} = H_1 + \frac{V_1^2}{2g} + k_{contraction}\frac{V_1^2}{2g} \quad (24)$$

The four equations (Continuity, Energy, C^+ and C^-) are solved simultaneously to get the pressure head and flow velocity at the downstream end of the upstream pipe and at the upstream end of the downstream pipe.

For reverse flow, the energy equation is:

$$H_1 + \frac{V_1^2}{2g} = H_n + \frac{V_n^2}{2g} + k_{expansion}\frac{V_1^2}{2g} \quad (25)$$

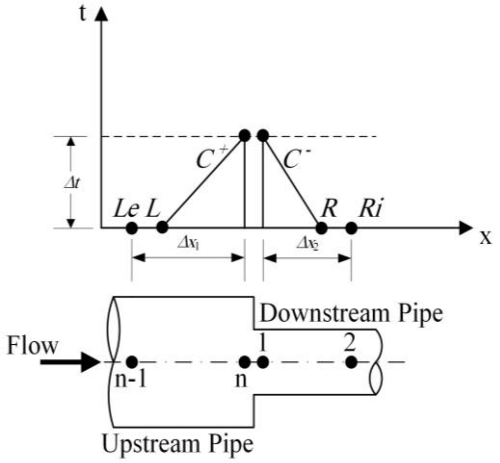

Fig. 4. Characteristic lines for series pipe junction

III. EXPERIMENTAL SETUP

The isometric view of the test rig used to carry out the water hammer experiment is shown in Fig. 5. It mainly represents an air-over-water pressure tank, pipe and valve system. The test rig starts with a water tank of 2.5 m^3 that holds water and compressed air to have a system like "reservoir" where its head remains almost constant. The water tank is followed by the isolation valve that used to isolate the main pipeline from the tank. After the isolation valve, a pressure transducer is placed to measure the pressure at the upstream end of the pipeline. At the end of the 23.8 m Polyvinyl chloride (PVC) pipeline, there exists the pressure transducer to record the pressure signal generated by the closure of the solenoid valve which is located after the pressure transducer.

Figure 6 shows the assumed variation of the minor loss coefficient of the solenoid valve. Downstream the solenoid valve, a ball valve is mounted to adjust the flow rate. The flow rate of water is measured by weighing the mass of water collected within a certain time. Pressure transducer signals are saved via OMEGA data logger (Type: OM-DAQ-USB-2401) and the signals are filtered using the Fourier Transform to eliminate the redundant frequencies that distort the desirable data.

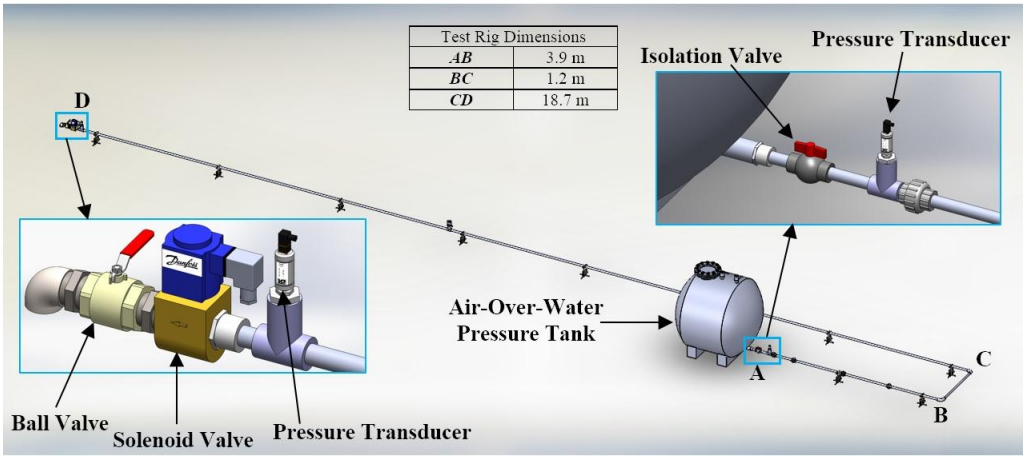

Fig. 5. Isometric view of water hammer test rig

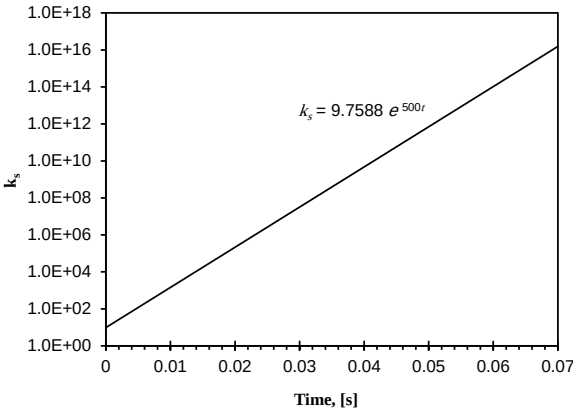

Fig. 6. Variation of solenoid valve minor loss coefficient, k_s, with time (Logarithmic vertical axis)

IV. Experimental Cases

Four experimental cases are used to validate the numerical code; two of them are from the literature and the others are the present study experimental work. The cases are for single pipe and three pipes in series.

Case of single pipe (*Kodura and Weinerowska* [16])

The first experiment used to validate the code in case of single pipe was performed by **Kodura and Weinerowska [16]** in the Laboratory of the Institute of Water Supply and Water Engineering of Warsaw University of Technology. It is represented by the schematic diagram in Fig. 7, and the specifications are given in Table 2.

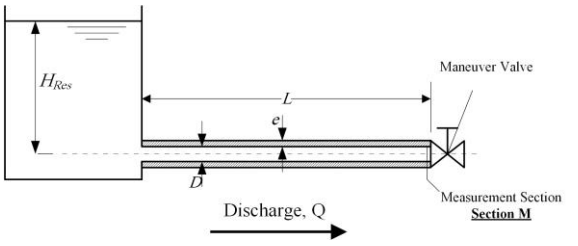

Fig. 7. Single pipe schematic diagram (Reservoir-Pipeline-Valve)

TABLE 2
SPECIFICATIONS OF THE EXPERIMENT CARRIED OUT BY KODURA AND WEINEROWSKA [16]

Specification	Value
Pipe material	MDPE
Length, L [m]	36
Internal diameter, D [mm]	40.8
Wall thickness, e [mm]	4.6
Roughness, [mm]	0.004
Poisson ratio, υ	0.46
Retardation time, τ [s] (Ref. [17])	0.0541
Creep coefficient, J [10^{-10} Pa^{-1}] (Ref. [17])	0.9
Reservoir head, H_{Res} [m]	39.2
Valve closure time, t_c [s]	0.024
Wave celerity, a [m/s]	423
Steady flow rate, Q [l/s]	0.744

In their experiment, the pipe was fed with water from large reservoir where the pressure was constant to a certain value. At the downstream end of the pipe, there was a ball valve mounted used to generate the transient flow by closing it suddenly and its closure time was measured with a precise electronic stop watch connected to the valve.

Case of three pipes in series (*Meniconi et al.* [1])

Figure 8 illustrates a schematic diagram of pipeline with a partial blockage. The experiment used to validate the code in case of three pipes is carried out by **Meniconi et al. [1]**. Its specifications are presented in Table 3.

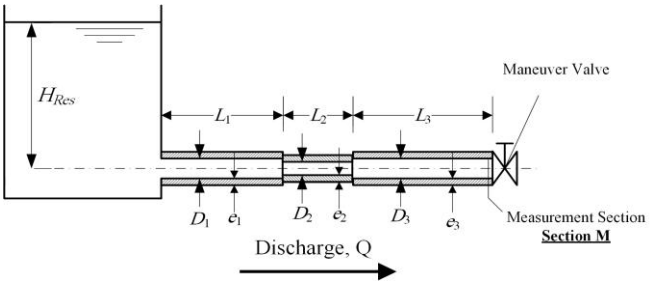

Fig. 8. Three pipes in series schematic diagram (Pipeline with extended blockage)

TABLE 3.
SPECIFICATIONS OF THE EXPERIMENT CARRIED OUT BY MENICONI ET AL. [1]

Specification	Pipe 1	Pipe 2	Pipe 3
Pipe material	HDPE		
Length, L [m]	54.49	6.6	110.44
Internal diameter, D [mm]	93.3	38.8	93.3
Wall thickness, e [mm]	8.1	3.9	8.1
Young's modulus, E [10^9 Pa]	2.2	2.62	2.2
Poisson ratio, υ	0.46	0.46	0.46
Reservoir head, H_{Res} [m]	21.1		
Valve closure time, t_c [s]	0.08		
Pressure wave celerity, a [m/s]	377.15	431.38	377.15
Retardation time, τ [s]	0.13	0.08	0.13
Creep coefficient, J [10^{-10} Pa^{-1}]	1.176	3.817	1.176
Steady flow rate, Q [l/s]	2.2		

Case of single pipe (*Present study*)

The test rig used is shown in Figure 5. The total length of the PVC pipeline is 23.8 m and internal diameter of 25 mm with wall thickness equals to 4.2 mm. The specifications of the water and pipe used in the calculation of wave celerity are given in Table 4. Both retardation time and creep coefficient of PVC pipe are reported by **Soares et al. [18]**.

Case of three pipes in series (*Present study*)

The test rig in Fig. 5 is modified to include three pipes in series. The second pipe is inserted after 0.42 m "Run T1" and 1.9 m "Run T2" from the upstream end of the pipe and its length is 0.43 m. It has the same material properties of 25 mm internal diameter pipe; except its internal diameter is 15.8 mm and its wall thickness is 2.77 mm. The total length of the pipes remains fixed at 23.8 m in the runs. The specifications of the three pipes runs are given in Table 5.

TABLE 4.
SPECIFICATIONS OF THE PRESENT STUDY WATER HAMMER TEST RIG AND SINGLE PIPE RUN

Specification		Value
Pipe material		PVC
Water bulk modulus, K [Pa]		2.15 x 10^9
Water density, ρ [kg/m^3]		998.2
Pipe material Young modulus, E [10^9 Pa]		2.4
Pipe internal diameter, D [mm]		25
Pipe wall thickness, e [mm]		4.2
Poisson ratio, υ		0.4
Retardation time, τ [s] (Ref. [18])		0.05
Creep coefficient, J [10^{-10} Pa^{-1}] (Ref. [18])		0.225
Constraint coefficients, ψ	(a)	0.85
	(b)	0.84
	(c)	1
Pressure wave celerity, a [m/s] "Calculated"	(a)	623.95
	(b)	626.98
	(c)	583.21
Single Pipe Run "Run S1":		
Steady flow rate, Q [m^3/s]		1.59 x 10^{-4}
Flow velocity, V_0 [m/s]		0.324
Reynolds number, R_e		8097.8
Reservoir head, H_{Res} [m]		32.45
Pipe length, L [m]		23.8
Wave celerity, a [m/s] "Calibrated"		622

TABLE 5.
SPECIFICATIONS OF THE PRESENT STUDY THREE PIPES IN RUNS T1 AND T2

Dimensional Parameter	Run T1	Run T2
First pipe length, L_1 [m]	0.42	1.9
Second pipe length, L_2 [m]	0.43	0.43
Third pipe length, L_3 [m]	22.95	21.47
Steady flow rate, Q [m^3/s]	2.3 x 10^{-4}	1.2 x 10^{-4}
Reynolds number, R_{e1}	11713.8	6111.5
Reservoir head, H_{Res} [m]	28.056	14.86
a [m/s] "Calibrated" D = 25 mm	622	622
a [m/s] "Calculated" D = 15.8 mm	638	638

V. RESULTS AND DISCUSSION

A. *Model Validation*

The developed code is validated by comparing its output results with the four experimental case studies in case of either single pipe or three pipes in series.

Case of single pipe (*Kodura and Weinerowska* [16])

Figure 9 shows the comparison between the results obtained from the developed mathematical code and the experimental data resulted from the experiment carried out by **Kodura and Weinerowska [16]**. It is obvious that the developed code predicts the maximum and minimum values of the pressure head fluctuations satisfactory. However, there is a slight phase shift.

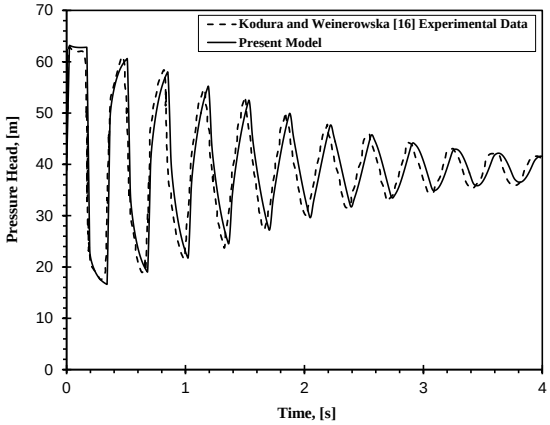

Fig. 9. Comparison between the present model results and the experimental data of Kodura and Weinerowska [16] at section M

***Case of three pipes in series* (*Meniconi et al.* [1])**

Figure 10 shows the comparison between the present model results with **Meniconi et al. [1]** numerical and experimental results. From Figure 10, the results obtained from the present model matches with good agreement the numerical results of **Meniconi et al. [1]**.

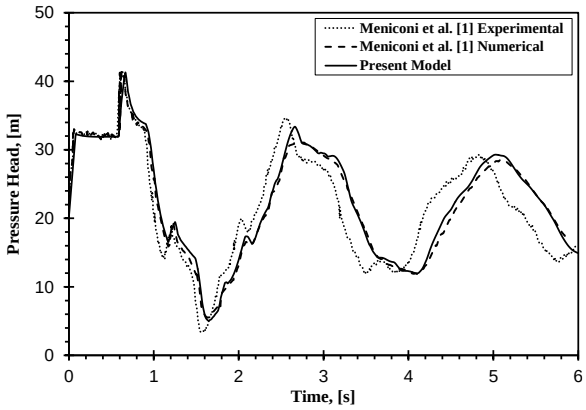

Fig. 10. Comparison between the present model results and both experimental and numerical data of Meniconi et al. [1] at section M

The previous discussion presents the validation of the developed code with two experimental data in case of single and partial blockage viscoelastic pipes and the comparisons show a good reliability of the code results.

***Case of single pipe* (*Present study*)**

The comparison between the present model and present experimental data, Figure 11, shows a good match in predicting the maximum and minimum values of the pressure head. The phase shift is not obvious, as the value of pressure wave celerity is calibrated to a certain value as illustrated in Table 4. The figure shows also a good prediction of the damping behavior of the pressure wave when using the proposed creep function by **Soares et al. [18]**. In addition, the assumed variation of the minor loss coefficient of the solenoid valve works well. The difference in the pressure wave profile between the present experimental data and numerical results is ascribed to neglecting the total effect of fluid-structure interaction in the mathematical model.

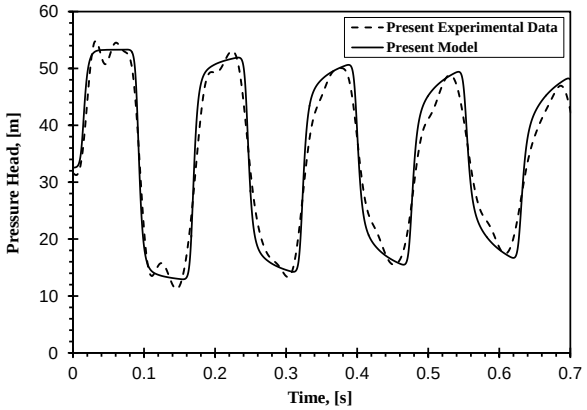

Fig. 11. Comparison between present model data and present experimental data at section M (Single pipe "Run S1")

***Case of three pipes in series* (*Present study*)**

In the case of the pipeline with a partial blockage, Figures 12 and 13 illustrate both experimental data and numerical data obtained from the developed code. From the two figures, they reveal that the code overpredicits the maximum and minimum values of the pressure head, in addition to a phase shift which arises after the second peak and increases progressively.

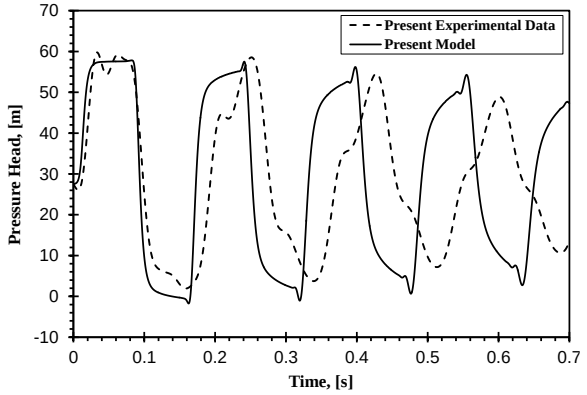

Fig. 12. Comparison between present model data and present experimental data at section M (Three pipes in series "Run T1")

It is worth noting that from the numerical and experimental results of **Meniconi et al. [1]**, Figure 10, there is a phase shift between the results. This may be attributed to that the 1D model is not able to take into account the graduality change in flow velocity across the abrupts "junctions". Therefore, it is preferable to use a 2D model to simulate the water hammer for complex systems that include junctions such as abrupts or develop a 1D model that can simulate that phenomenon with more accurate results. Neglecting the total effect of fluid-structure interaction (FSI) can also be added to the aforementioned causes which lead to less qualitative agreement between the experimental and numerical results.

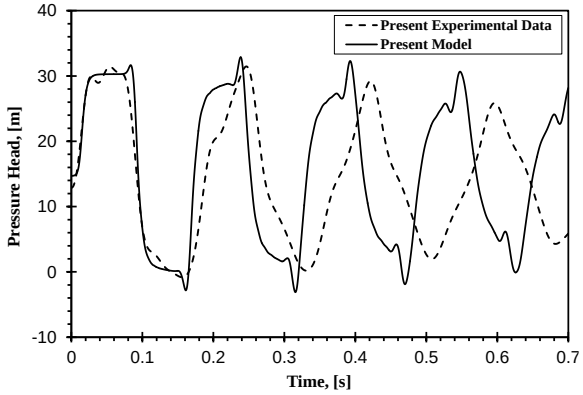

Fig. 13. Comparison between present model data and present experimental data at section M (Three pipes in series "Run T2")

B. Sensitivity Analysis

In this section, some parameters are studied to investigate its effects on water hammer pressure fluctuations and maximum pressure head for both cases; single pipe and three pipes. The numerical results obtained in Figures 11 and 13 are used to clarify the effect of changing the studied parameters. "Run S1" is referred to the numerical results of single pipe and "Run T2" referred to the numerical results of three pipes.

Single Pipe

The effects of the flow velocity, pipeline length, pipe size, pipe material, and valve closing protocol on the water hammer are studied numerically.

1. *Effect of flow velocity*

The effect of flow velocity variation on the water hammer is studied using the three runs S1, S2 and S3, Table 7. The effect of flow velocity on the pressure head is illustrated in Figure 14. Based on the numerical results, the maximum calculated pressure heads, $\max.H_{num}$, the maximum pressure head rise at the valve, $\Delta H_{\max}$, ($\Delta H_{\max} = \max.H_{num}$ – Steady pressure head at the valve) and the flow velocity, V_0, are: $\max.H_{num}$ = {53.31; 73.83; 43.04} m, $\Delta H_{\max}$ = {20.75; 41.79; 10.34} m, and V_0 = {0.324; 0.648; 0.162} m/s for "Run S1", "Run S2" and "Run S3", respectively. For the same pipe, increasing the flow velocity of water increases the pressure head rise in transient event.

TABLE 7.
DATA USED IN RUNS S1, S2 AND S3

Dimensional Parameter	Run S1	Run S2	Run S3
Flow velocity, V_0 [*m*/*s*]	0.324	0.648	0.162
Reynolds number, Re	8097.8	16195.6	4048.9

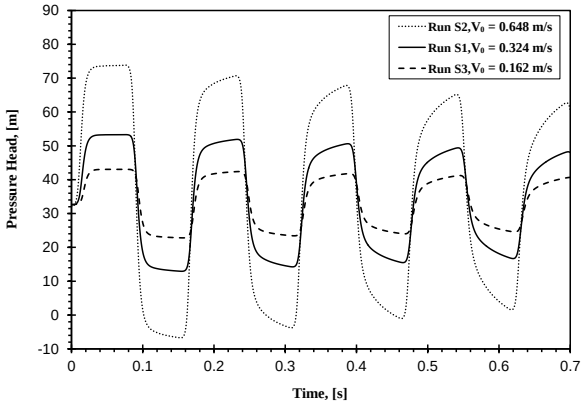

Fig. 14. Influence of flow velocity on water hammer pressure wave profile

2. *Effect of pipeline length*

The effect of pipeline length variation on the water hammer is studied using the three runs S1, S4 and S5, Table 8. From Figure 15, shorter pipe leads to large value of pressure wave frequency. As the period of pressure wave equals 4*L/a*, decreasing pipe length leads to a small wave period. The maximum calculated pressure heads are: $\max.H_{num}$ = {53.31, 53.26, 53.21} m and $\Delta H_{\max}$ = {20.75, 20.82, 20.56} m, for "Run S1", "Run S4" and "Run S5", respectively. Run S5 has the minimum pressure head rise because the reflection time of the pressure wave is less than the valve closure time, and if the length is reduced to 5 meters, the pressure head rise becomes 18 m. The damping of the pressure wave is greater with decreasing the pipe length.

TABLE 8.
DATA USED IN RUNS S1, S4 AND S5

Dimensional Parameter	Run S1	Run S4	Run S5	Run S5'
Length, *L* [*m*]	23.8	40	10	5

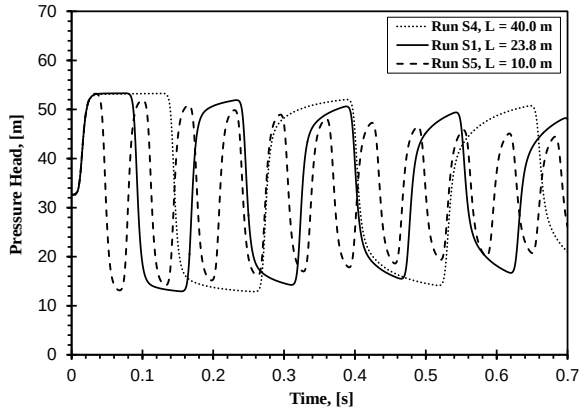

Fig. 15. Influence of pipeline length on water hammer pressure wave profile

3. *Effect of pipe size*

The effect of pipe size on the water hammer is studied using the three runs S1, S6 and S7, Table 9. Pipe dimensions are investigated by assuming that the pipeline is 15.8 mm internal diameter "Run S6" and 49.25 mm internal diameter "Run S7". As presented in Figure 16, the smaller pipe has the maximum pressure head rise and vice versa. These results agree with that obtained by **Emadi and Solemani [4]** and **Mansuri et al. [5,6]**. This is attributed to the high values of the water flow velocity, for constant discharge, and the pressure wave celerity.

TABLE 9.
DATA USED IN RUNS S1, S6 AND S7

Dimensional Parameter	Run S1	Run S6	Run S7
Internal diameter, D [mm]	25	15.8	49.25
Wall thickness, e [mm]	4.2	2.77	5.54
Wave celerity, a [m/s]	622	638.51	529.56
Flow velocity, V_0 [m/s]	0.324	0.811	0.0835
Reynolds number, Re	8097.8	12812.98	4110.56

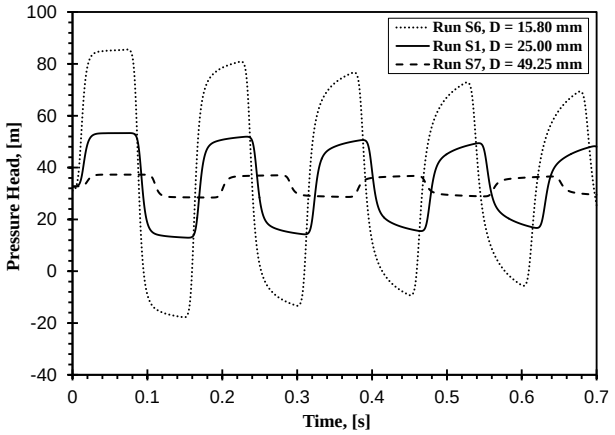

Fig. 16. Influence of pipeline dimensions on water hammer pressure wave profile

4. *Effect of pipe material*

The effect of pipe material is studied by replacing the PVC pipe by a High-density polyethylene (HDPE) pipe. Table 10 gives the properties of HDPE pipe reported by **Covas et al. [8]**. They have different properties (Young's modulus, Poisson ratio, creep compliance, and retardation times).

Figure 17 shows that changing pipe material results in slower wave celerity and that lead to longer period and low frequency. As the HDPE pipe has more viscoelasticity behavior than the PVC pipe, as shown in Figure 18, more damping for the pressure wave is generated.

TABLE 10. PROPERTIES OF PVC AND HDPE PIPES USED IN RUNS S1 AND S8

Dimensional Parameter	Run S1	Run S8				
Material	PVC	HDPE				
Young's modulus, E [10^9 Pa]	2.4	1.43				
Poisson ratio, υ	0.4	0.46				
Retardation time, τ [s]	0.05	0.05	0.5	1.5	5	10
Creep coefficient, J [10^{-10} Pa^{-1}]	0.225	1.057	1.054	0.9051	0.2617	0.7456
Wave celerity, a [m/s]	622	517.08				

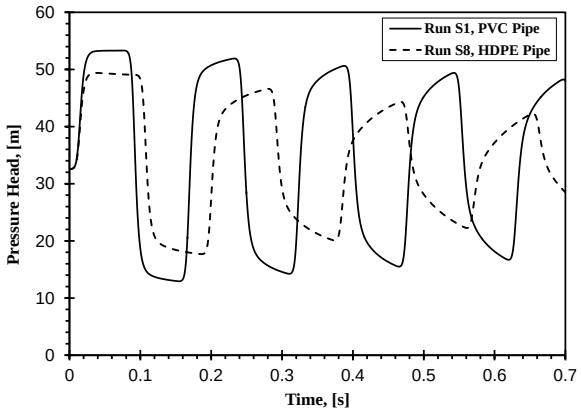

Fig. 17. Influence of pipeline material on water hammer pressure wave profile

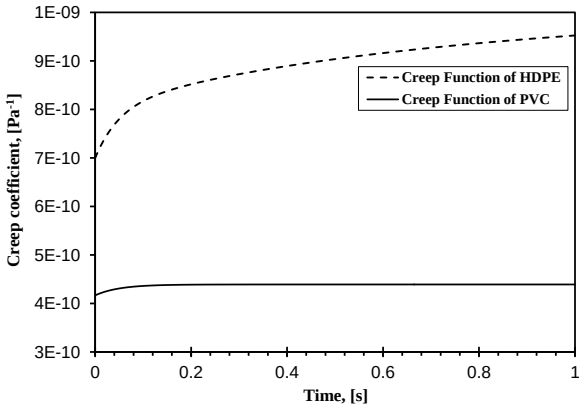

Fig. 18. Creep functions of HDPE and PVC pipes

5. *Effect of valve closing protocol*

The effect of the valve closing protocol is studied by achieving Runs S1, S9, S10 and S11, Table 11.

Figure 19 shows the effect of the valve closing protocol on the water hammer. Referring to Fig. 19(c), it is observed that for linear closing (Run S11), the pressure head rise linearly as well.

On the other hand, in case of the instantaneous closing, Fig. 19(a), as a result of the sudden stoppage of water velocity, the pressure head rises instantaneously at the beginning of the transient event (at t= 0 s). Figure 19(b) demonstrates that there is a little increase in pressure head until 0.07 second "valve closure time", then the rise of pressure head is increased rapidly. In general, there is a phase shift in each figure despite that there is neither change in pressure wave celerity value nor change in pipeline length. This refers to the important role the valve contributes in forming pressure fluctuation profile.

TABLE 11.
DATA USED IN RUNS S1, S9, S10 AND S11

Run	Closing Protocol
S1	Solenoid valve minor loss coefficient $k_s = 9.5788\, e^{500t}$
S9	Instantaneous (Closure time t_c = 0 s)
S10	Solenoid valve minor loss coefficient $k_s = 9.5788\, e^{10t}$
S11	Velocity decreasing linearly

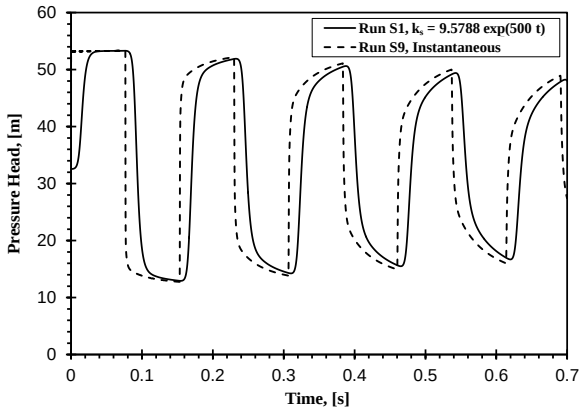

(a)

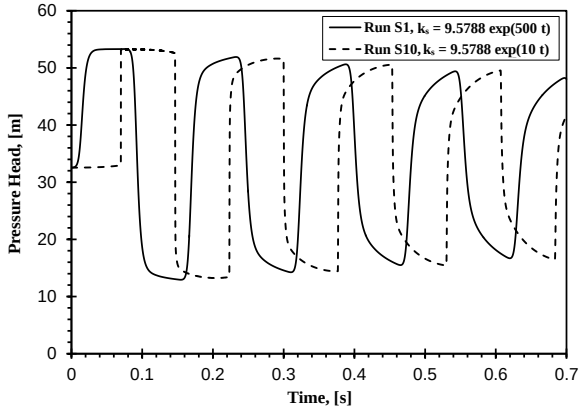

(b)

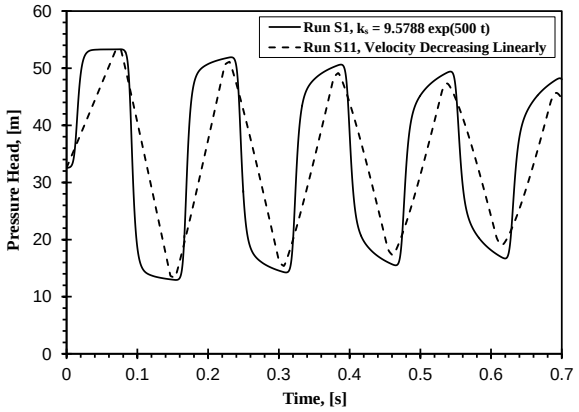

(c)

Fig. 19. Influence of closing protocol of solenoid valve on water hammer pressure wave profile

Three Pipes in Series

The effects of the location and length of the small size pipe representing blockage are explained.

1. *Effect of location*

The effect of the small size pipe (L_2 = 0.43 m) location on the water hammer is investigated using the data of Runs T2, T3 and T4, Table 12. The total length of the pipes is constant at 23.8 m in all runs.

Figure 20 illustrates that the change of the small size pipe location changes the instance when the pressure spike, which results from the reflected pressure wave at the abrupt contraction, appears. That is clear from the first peak, the nearer the pipe from the valve, the earlier the spike appears.

TABLE 12.
DATA USED IN RUNS T2, T3 AND T4

Run	Location
T2	At 1.9 m from upstream end of the pipe (L_1 = 1.9 m, L_3 = 21.47 m)
T3	At 11.7 m from upstream end of the pipe (L_1 = 11.7 m, L_3 = 11.67 m)
T4	At 1.9 m from downstream end of the pipe (L_1 = 21.47 m, L_3 = 1.9 m)

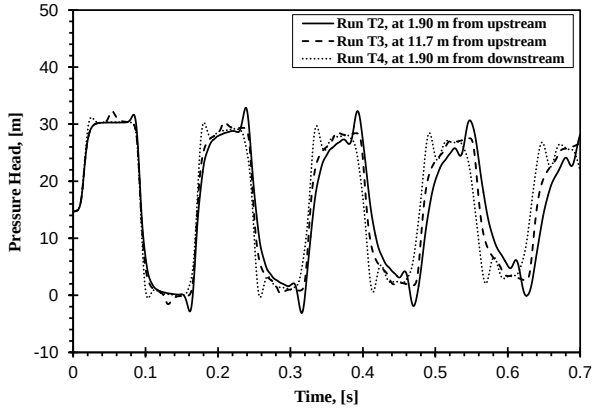

Fig. 20. Influence of blockage "L_2" location on water hammer pressure wave profile

2. ***Effect of blockage length***

The effect of the small size pipe length is evaluated by taking its length L_2=2 m (Run T5) instead of L_2=0.43m (Run T2) and L_2=1m (Run T6), but the first pipe length L_1=1.9m. The total length of the pipes is constant at 23.8 m, Table 13.

Figure 21 shows that the additional pressure rise occurred in the first peak of "Run T5" is higher than that occurred in "Run T2". That is because of the less intense overlapping of pressure waves transmitted and reflected by the abrupt expansion and the abrupt contraction, respectively.

TABLE 13.
DATA USED IN RUNS T2, T5 AND T6

Dimensional Parameter	Run T2	Run T5	Run T6
Blockage length, L_2 [m]	0.43	2.00	1.00
Third pipe length, L_3 [m]	21.47	19.9	20.9

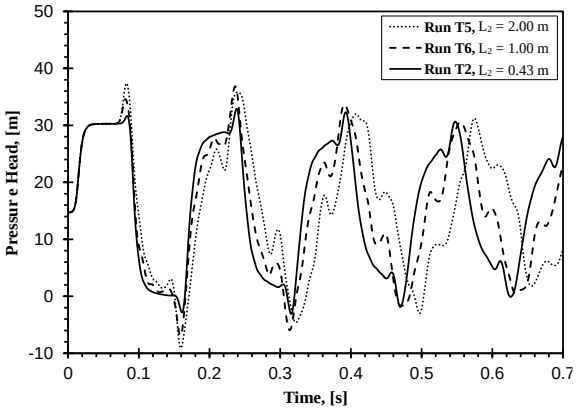

Fig. 21. Influence of blockage length "L_2" on water hammer pressure wave profile

VI. CONCLUSIONS

In the present paper, a mathematical model is developed to simulate water hammer in simple and in series viscoelastic pipes. The numerical results illustrated throughout this paper, are obtained from the MATLAB code taking into account the effect of pipe wall viscoelasticity and fluid unsteady friction and without considering the total effect of fluid-structure interaction. An equation describing the change of the minor loss coefficient of the solenoid valve, used in the present experimental work, is assumed to get better results. The code is validated in both cases (single pipe and three pipes in series) with the experimental data of **Kodura and Weinerowska [16]** and **Meniconi et al. [1]**, respectively. The code predicts the results satisfactorily. The code is also validated with experimental data extracted from the experiments conducted at the Hydraulic Machines Laboratory, Faculty of Engineering, Mansoura University. The Fourier transform is used to filter the pressure transducers signals. Finally, a sensitivity analysis is carried out to investigate the effect of some essential parameters on the pressure fluctuation. The outcome results are summarized as follows:

- Increasing the flow velocity and consequently the Reynolds number for a pipe, increases the pressure head rise when a transient event occurs.
- For shorter pipes, the frequency of the pressure wave is high beside the pressure head decreases if the characteristic time of the pipe ($2L/a$) is less than the closure time of the valve and the maximum pressure head generated depends also on the closing protocol of the valve.
- The small size pipes lead to increase in pressure wave celerity and so increase in pressure head rise.
- Closing protocol of the valve plays a vital role in determining the maximum pressure head generated and pressure wave profile.

For three pipes in series, the location of the small size pipe affects the instant when the spike, which resulted from the reflected pressure wave from the abrupt contraction, appeared in the first peak. When the length of the small pipe is increased, while the total length remains constant, the spike generated is higher in amplitude. This amplitude value depends also on the closing protocol of the valve and the characteristic time of the pipe ($2L/a$). In addition to that, the frequency of the pressure wave decreases for the same total length of the pipeline.

Finally, it is recommended to include the total effect of fluid-structure interaction (FSI) while studying the water hammer phenomenon, especially for systems that have various types of junctions and not rigidly fixed, in addition to developing a code that takes into account the effect of fluid graduality at abrupt.

REFERENCES

[1] Meniconi, S., Brunone, B., and Ferrante, M. (2012). Water-Hammer Pressure Waves Interaction at Cross-Section Changes in Series in Viscoelastic Pipes. Journal of Fluids and Structures, Vol. 33, pp. 44–58.

[2] Massari, C., Yeh, T.-C. J., Ferrante, M., Brunone, B., and Meniconi, S. (2015). A Stochastic Approach for Extended Partial Blockage Detection in Viscoelastic Pipelines: Numerical and Laboratory Experiments. Journal of Water Supply: Research and Technology—AQUA, Vol. 64, Issue 5, pp. 583–595.

[3] Meniconi, S., Brunone, B., Ferrante, M., and Capponi, C. (2016). Mechanism of Interaction of Pressure Waves at a Discrete Partial Blockage. Journal of Fluids and Structures, Vol. 62, pp. 33–45.

[4] Emadi, J. and Solemani, A. (2011). Maximum Water Hammer Sensitivity Analysis. World Academy of Science, Engineering and Technology, Vol. 5, No. 1, pp. 17–20.

[5] Mansuri, B., Salmasi, F., and Oghati, B. (2014). Effects of Pipe's Roughness and Reservoir Head Levels on Pressure Waves in Water Hammer. Journal of Civil Engineering and Urbanism, Vol. 4, Issue 1, pp. 36–40.

[6] Mansuri, B., Salmasi, F., and Oghati, B. (2014). Sensitivity Analysis for Water Hammer Problem in Pipelines. Iranica Journal of Energy and Environment, Vol. 5, Issue 2, pp. 124–131.

[7] MATLAB version R2014b, The MathWorks, Inc., Natick, Massachusetts, United states. https://www.mathworks.com/products/new_products/release2014b.html

[8] Covas, D., Stoianov, I., Mano, J., Ramos, H., Graham, N., and Maksimovic, C. (2005). The Dynamic Effect of Pipe-Wall Viscoelasticity in Hydraulic Transients. Part II— Model Development, Calibration and Verification. Journal of Hydraulic Research, Vol. 43, pp. 56–70.

[9] Keramat, A., Tijsseling, A. S., and Ahmadi, A. (2010). Investigation of Transient Cavitating Flow in Viscoelastic Pipes. IOP Conference Series: Earth and Environmental Science, Vol. 12, No. 1, p. 012081. IOP Publishing.

[10] Vardy, A., and Brown, J. (2004). Efficient Approximation of Unsteady Friction Weighting Functions. Journal of Hydraulic Engineering, ASCE, Vol. 130, No. 11, pp. 1097–1107.

[11] Fox, J. A. (1977). Hydraulic Analysis of Unsteady Flow in Pipe Networks. First edition. The Macmillan Press Ltd.
[12] Watters, G. Z. (1984). Analysis and Control of Unsteady Flow in Pipelines. Second edition, Butterworth-Heinemann, USA.
[13] Wylie, E. B. and Streeter, V. L. (1993). Fluid Transients in Systems. Prentice Hall, Englewood Cliffs, NI.
[14] Larock, B. E., Jeppson, R. W., and Watters, G. Z. (2000). Hydraulics of Pipeline Systems. New York: CRC Press LLC.
[15] Chaudhry, M. H. (2014). Applied Hydraulic Transients. Third edition. Springer.
[16] Kodura, A. and Weinerowska, K. (2005). The Influence of the Local Pipe Leak on the Properties of the Water Hammer. Proc. of 2nd Congress of Environmental Engineering, Lublin, Poland, Vol. 1, pp. 399–407.
[17] Weinerowska-Bords, K. (2006). Viscoelastic Model of Waterhammer in Single Pipeline – Problems and Questions. Archives of Hydro-Engineering and Environmental Mechanics, Vol. 53, pp. 331–351.
[18] Soares, A., Covas, D., and Reis, L. (2008). Analysis of PVC Pipe-Wall Viscoelasticity during Water Hammer. Journal of Hydraulic Engineering, ASCE, Vol. 134, pp. 1389–1394.